Biogeochemistry (2022) 160:17–33
https://doi.org/10.1007/s10533-022-00937-5

Contributions of Fe(III) to UV–Vis absorbance in river water: a case study on the Connecticut River and argument for the systematic tandem measurement of Fe(III) and CDOM

Laura A. Logozzo · Joseph W. Martin · Johnae McArthur · Peter A. Raymond

Received: 24 September 2021 / Accepted: 22 April 2022 / Published online: 16 May 2022
© The Author(s) 2022

Abstract Dissolved organic matter (DOM) impacts the structure and function of aquatic ecosystems. DOM absorbs light in the UV and visible (UV–Vis) wavelengths, thus impacting light attenuation. Because absorption by DOM depends on its composition, UV–Vis absorbance is used to constrain DOM composition, source, and amount. Ferric iron, Fe(III), also absorbs in the UV–Vis; when Fe(III) is present, DOM-attributed absorbance is overestimated. Here, we explore how differing behavior of DOM and Fe(III) at the catchment scale impacts UV–Vis absorbance and evaluate how system-specific variability impacts the effectiveness of existing Fe(III) correction factors in a temperate watershed. We sampled five sites in the Connecticut River mainstem biweekly for ~ 1.5 years, and seven sites in the Connecticut River watershed once during the summer 2019. We utilized size fractionation to isolate the impact of DOM and Fe(III) on absorbance and show that variable contributions of Fe(III) to absorbance at 254 nm (a_{254}) and 412 nm (a_{412}) by size fraction complicates correction for Fe(III). We demonstrate that the overestimation of DOM-attributed absorbance by Fe(III) is correlated to the Fe(III):dissolved organic carbon concentration ratio; thus, overestimation can be high even when Fe(III) is low. a_{254} overestimation is highly variable even within a single system, but can be as high as 53%. Finally, we illustrate that UV-Vis overestimation might impart bias to seasonal, discharge, and land-use trends in DOM quality. Together, these findings argue that Fe(III) should be measured in tandem with UV–Vis absorbance for estimates of CDOM composition or amount.

Keywords Carbon · Dissolved organic matter · CDOM · Rivers · UV–Vis absorbance · Iron · Water color

Supplementary Information The online version contains supplementary material available at https://doi.org/10.1007/s10533-022-00937-5.

L. A. Logozzo (✉) · J. McArthur · P. A. Raymond
School of the Environment, Yale University, New Haven, CT, USA
e-mail: laura.logozzo@yale.edu

J. W. Martin
U.S. Geological Survey, Hartford, CT, USA

J. McArthur
Department of Political Science, University of Connecticut, Storrs, CT, USA

Introduction

UV and visible (UV–Vis) light absorption in aquatic systems is commonly measured to elucidate dissolved organic matter (DOM) source, composition, and amount, and yet light absorption in the same wavelengths by iron complicates DOM characterization. DOM modulates the structure and function of aquatic ecosystems. Within aquatic ecosystems,

both the amount of DOM and its chemical composition determines its role. DOM influences the transport, removal, and availability of trace metals from aquatic systems through complexation, with greater complexation associated with DOM of higher aromaticity (Baken et al. 2011; Kikuchi et al. 2017). While DOM fuels heterotrophic production in aquatic systems (Wetzel 1992), DOM composition affects DOM availability to microbes, and therefore, the extent of its contribution to metabolism (Benner 2003). Because the colored component of DOM, colored dissolved organic matter (CDOM), absorbs light, it limits the amount of UV radiation and visible light in aquatic systems and affects water color (Bricaud et al. 1981); however, the amount of light absorption by CDOM is dependent on its concentration and composition, with differing light absorbing characteristics associated with DOM of different sources. Thus, UV–Vis absorbance can also be used to constrain DOM amounts, sources, and composition.

UV–Vis absorbance is a powerful tool for characterizing DOM chemical composition, or "quality," and amount in aquatic systems. For example, Hernes and Benner (2003) found the DOM absorption coefficient at 350 nm (a_{350}) to be associated with dissolved lignin concentration. DOM molecular weight can be approximated using the log-transformed absorption slope from 275 to 295 nm ($S_{275–295}$) or the slope ratio (S_R), which is the ratio of the slopes at 275–295 nm and 350–400 nm (Helms et al. 2008). Additionally, $S_{275–295}$ is often used in remote sensing algorithms to estimate DOC concentrations (Fichot and Benner 2011; Cao et al. 2018). DOC or CDOM amount can also be quantified from satellite imagery by estimating absorbance in the visible wavelengths, such as at 412 nm (a_{412}) (Mannino et al. 2014; Alcântara et al. 2017; Zhang et al. 2021), and correlating this to DOC concentration. Finally, DOM aromaticity is commonly approximated using the specific UV absorbance at 254 nm ($SUVA_{254}$), which is the absorption of DOM at 254 nm (a_{254}) divided by the DOC concentration (Weishaar et al. 2003); DOM aromaticity is a widely used parameter to determine the potential for the formation of carcinogenic disinfectant byproducts during water treatment (Kitis et al. 2002), as a predictor for trace metal complexation (Baken et al. 2011; Kikuchi et al. 2017), and as a proxy for DOM source. The advancement in these methods and analyses has allowed for a more comprehensive analysis of DOM quality and quantity across a variety of systems and at higher frequencies due to the speed and cost-efficiency of the methods.

DOM is operationally defined by discrete filter pore size cut-offs (< 0.22 to < 0.7 µm), and thus CDOM optical measurements are commonly performed on 0.22 µm filtrate. However, UV–Vis absorption by chemical species other than DOM has been acknowledged (Weishaar et al. 2003; Xiao et al. 2013; Poulin et al. 2014). The other dominant dissolved species that absorbs in similar wavelengths to DOM is iron. If iron is not measured, contributions of iron to UV–Vis absorbance can be mistaken for absorption by DOM, thereby introducing error to absorbance measurements at wavelengths where numerous DOM parameters are calculated (e.g., a_{254}, a_{412}, $SUVA_{254}$). While total dissolved iron in natural waters is composed of ferric and ferrous iron, Fe(III) and Fe(II), respectively, in general, iron absorption has been attributed to Fe(III), while the absorption of Fe(II) has been shown to be small relative to Fe(III) (Maloney et al. 2005) or negligible (Poulin et al. 2014).

Fe(III) UV–Vis absorption has been shown to increase linearly with Fe(III) concentration (Weishaar et al. 2003; Xiao et al. 2013; Poulin et al. 2014). Thus, studies that wish to report only the contribution of DOM to UV–Vis absorbance can correct for Fe(III) contributions to total UV–Vis absorbance by using the measured Fe(III) concentration and a wavelength-specific Fe(III) coefficient (i.e., a correction factor) developed by Poulin et al. (2014). However, while total iron and Fe(II) concentrations can be easily measured, Fe(III) concentrations, and therefore, the contributions of Fe(III) to UV–Vis absorbance, are rarely measured and reported in studies that aim to examine DOM quantity and quality using DOM UV–Vis absorption. This may be because measurements of Fe(III) concentrations are time-sensitive due to the rapid oxidation of Fe(II) in oxygenated circumneutral waters, and because the importance of iron correction in natural waters is reportedly variable. Therefore, reported values of DOM-attributed UV–Vis absorbance are likely overestimated in some systems.

While some studies have shown that the absorption of iron significantly contributes to UV–Vis absorbance and water color (Maloney et al. 2005; Kritzberg and Ekström 2012; Xiao et al. 2013, 2015;

Poulin et al. 2014; Weyhenmeyer et al. 2014), others have shown that the contributions of iron to UV–Vis absorbance for iron concentrations typical of surface waters are negligible relative to the contributions of DOM (Weishaar et al. 2003; Asmala et al. 2012; Brezonik et al. 2019), indicating variability across systems. One potential driver for this variability is the ratio of iron to organic carbon, as this was observed to be highly correlated to the percent contribution of iron to water color in Finnish rivers (Xiao et al. 2015) and the Upper Great Lakes (Brezonik et al. 2019). Because both Fe(III) and DOM concentration and source have been shown to be driven by river discharge (Gaffney et al. 2008; Raymond and Saiers 2010; Ingri et al. 2018), season (Ingri et al. 2006; Shultz et al. 2018), and land use (Xiao et al. 2015), quantifying the impact of these factors on Fe(III) contributions to UV–Vis absorbance is necessary to determine when Fe(III) correction to UV–Vis DOM measurements might be essential and when Fe(III) absorption might be negligible. This is also particularly useful to retroactively evaluate potential Fe(III) interference in studies where DOM absorption coefficients or $SUVA_{254}$ values are presented without also presenting Fe(III) concentrations or without Fe(III) correction.

The contribution of Fe(III) to UV–Vis absorbance per Fe(III) concentration might also be more variable than previously reported. Fe(III) absorption depends on its speciation (Sherman and Waite 1985; Stefánsson 2007; Loures et al. 2013) as well as its source (Poulin et al. 2014), and thus a single wavelength-specific coefficient to correct for Fe(III) contributions to UV–Vis absorbance in DOM measurements, as proposed in Poulin et al. (2014), may not sufficiently account for Fe(III) absorption variability in natural waters. One method of constraining differences in Fe(III) UV–Vis absorption by speciation and source is by using size fractionation. The operationally dissolved fraction (< 0.22 µm) can be further separated by sequential filtration through a 0.02 µm filter into the truly dissolved, or soluble, fraction (< 0.02 µm) and the colloidal fraction (0.02 to 0.22 µm) (Gledhill and Buck 2012). Iron is distributed in both fractions, and the two size fractions of iron have been shown to have different chemical and physical properties, different speciation, and are derived from different sources (Ingri et al. 2006). Therefore, differences in the contribution of Fe(III) to UV–Vis absorbance due to differences in speciation or source canbe quantified using size fractionation.

Previous work has evaluated the contributions of dissolved ferric iron to dissolved UV–Vis absorbance in controlled lab experiments (Weishaar et al. 2003; Xiao et al. 2013; Poulin et al. 2014) and natural water samples (Xiao et al. 2013; Brezonik et al. 2019). These studies provide methods for determining the contribution of iron to UV–Vis absorbance. Yet, as we demonstrate here, constraining the contrasting influence of ferric iron and CDOM on UV–Vis absorbance in natural water samples is still prone to complications and demands further study. We find here that system-specific variability is important to understanding the contrasting influence, even in some systems with low ferric iron. Factors such as the size fraction of ferric iron and the Fe(III):DOC ratio, which can be impacted by river flow and land cover, can impart variability to the relative importance of ferric iron and CDOM. As such, we argue that although correction factors are useful, studies using UV–Vis absorbance to characterize DOM should systematically measure and present Fe(III) concentrations.

Materials

Sampling sites

Five sites along a 214 km stretch of the Connecticut River mainstem were sampled every other week from July 2018 to March 2020 (Table 1, Fig. 1a). All sites are actively monitored U.S. Geological Survey (USGS) stream gages with stage, temperature, pH, dissolved oxygen, conductivity, turbidity and fluorescent DOM measured every 15 min, and two out of the five sites, Thompsonville and Middle Haddam, report discharge every 15 min (U.S. Geological Survey 2021). Measurements of instantaneous discharge at the time of sampling were also available for samples collected at Northfield (U.S. Geological Survey 2021). In addition to the bi-weekly sampling along the Connecticut River mainstem, seven sites ranging from headwaters to large rivers throughout the Connecticut River watershed were sampled once synoptically over two days during the summer 2019, from 8/28 to 8/29 (Table 2, Fig. 1b). The sub-basin boundaries for each site was determined using StreamStats

Table 1 Sites along the Connecticut River mainstem sampled bi-weekly

Site	Location	USGS ID	Latitude	Longitude	Number of Samples	Median number of days between collection and 0.02 µm filtration[a]
NORT	Northfield, MA	01161280	42.68333	−72.47194	29	3 (8)
THOM	Thompsonville, CT	01184000	41.98722	−72.60583	29	2 (7)
HADD	Middle Haddam, CT	01193050	41.54167	−72.55361	29	1 (6)
ESSX	Essex, CT	01194750	41.35148	−72.38437	31	1 (4)
OLYM	Old Lyme, CT	01194796	41.31250	−72.34639	31	1 (4)

[a]Maximum number of days between sample collection and 0.02 µm filtration in parentheses

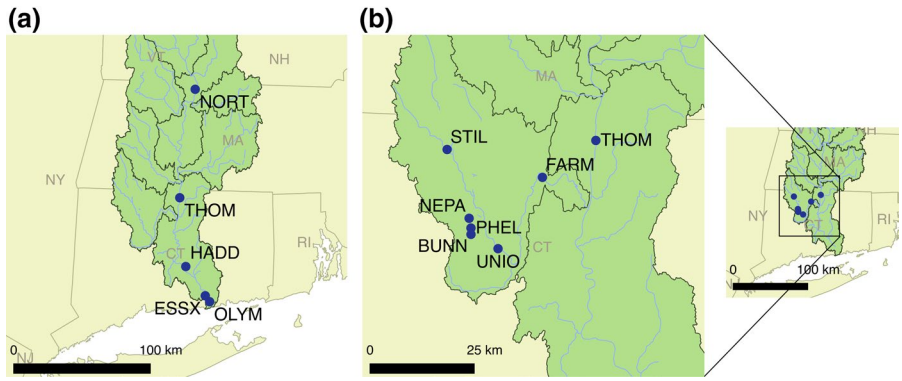

Fig. 1 The Connecticut River watershed (green) with **a** five sites along the Connecticut River mainstem sampled every two weeks and **b** seven sites sampled once during the summer 2019. Connecticut River watershed and sub-basin boundaries from U.S. Geological Survey (2022)

Table 2 Connecticut River watershed sites sampled once during the summer 2019

Site (4-letter code)	USGS ID	Latitude	Longitude	Drainage area (km^2)	Forest (%)	Wetland (%)	Agriculture (%)	Developed (%)
Bunnell Brook (BUNN)	01188000	41.78621	−72.96483	10.6	66.2	9.8	10.3	11.5
Farmington River Tariffville, CT (FARM)	01189995	41.90828	−72.75935	1494.0	70.2	8.1	3.2	14.3
Nepaug River (NEPA)	01187800	41.82065	−72.97010	61.6	78.0	7.2	5.9	7.4
Phelps Brook (PHEL)	01187830	41.79978	−72.96488	6.5	71.4	15.0	5.5	7.3
Still River (STIL)	01186500	41.96792	−73.03344	220.2	77.6	8.4	2.2	8.6
Connecticut River Thompsonville, CT (THOM)	01184000	41.98722	−72.60583	25,019.3	79.5	4.5	5.5	5.5
Farmington River Unionville, CT (UNIO)	01188090	41.75555	−72.88704	979.0	78.0	7.8	1.8	7.0

(Ries III et al. 2017). The percent land use for each designation was calculated for each sub-basin using the National Land Cover Database (NLCD) 2016 (available from www.mrlc.gov) in QGIS.

Sample collection and storage

Surface water samples were collected at each site using an acid-rinsed polypropylene bucket or jug, which was rinsed three times with sample water before collection. Samples were filtered on-site through Sterivex polyethersulfone membrane 0.22 µm filters (Sterivex #SVGP01050) using acid-washed PharMed BPT tubing and a peristaltic pump. All 0.22 µm filters and tubing were purged with at least 250 mL of milli-Q water, and then with at least 50 mL of sample. For Fe(II) collection in the Connecticut River mainstem bi-weekly sampling, an acid-washed Tygon E-3603 tube was attached to the outlet of a 0.22 µm filter and the tube placed in the bottom of an acid-washed 60 mL borosilicate glass amber bottle. The bottle was then over-filled three times with the 0.22 µm filtrate, the tube slowly removed, and the bottle capped immediately with PolyCone lined phenolic caps, ensuring that no air bubbles were trapped inside the sample bottle. This was placed immediately on ice, and then at 4 °C in the lab until further 0.02 µm sequential filtration and analysis. To collect water for operationally and truly dissolved total iron and DOM, two 120 mL HDPE bottles were filled with filtrate from the 0.22 µm filter immediately after collection on-site. Both samples were immediately placed on ice in the field and then at 4 °C in the lab until subsequent filtration and analysis. All sample bottles were acid-soaked with 1 N HCl for at least 24 hours and then rinsed four times with Milli-Q water prior to use.

0.02 µm filtration of CT River mainstem samples

Half (about 30 mL for ferrous iron and 120 mL for total iron/DOM) of the 0.22 µm sample for the Connecticut River mainstem sites was sequentially filtered through a Whatman Anopore inorganic membrane (Anodisc) 0.02 µm filter (Whatman # 89203-116) to separate the operationally dissolved fraction into the truly dissolved, or soluble, (<0.02 µm) and colloidal (0.02–0.22 µm) size fractions. All filtering equipment (e.g., vacuum flask) was acid-soaked in 1 N HCl, rinsed four times with milli-Q water, and then baked at 450 °C for five hours. The sequential filtration of a portion of the 0.22 um filtrate using the 0.02 µm filter was conducted on the Connecticut River mainstem samples within three days of collection for most samples (82%); however, some samples were filtered within three to seven days of collection due to the scheduling of sample pick-up and timing of high tide, and one sample was filtered after eight days of collection. In addition, the average amount of time between collection/0.22 µm filtration and 0.02 µm filtration varied by site due to our sampling strategy (Table 1). The 0.02 µm filters were placed on the vacuum filtration setup and rinsed with at least 300 mL of milli-Q water, and then with at least 10 mL of sample. Roughly 30 mL of the 0.22 µm Fe(II) filtrate was then 0.02 µm filtered, and Fe(II) was immediately measured on both size fractions. One of the two HDPE bottles containing 0.22 µm filtrate was then filtered through the 0.02 µm filter on the same vacuum setup, and transferred to a clean 120 mL HDPE bottle. The seven sites sampled as part of the summer 2019 sampling event were not 0.02 µm filtered.

Iron measurements

Fe(II) was measured using the 1,10-phenanthroline method (Hach Method 8146) on the Hach DR900 or the Hach FerroVer Pocket Colorimeter II immediately on-site after sampling and 0.22 µm filtering for the summer 2019 sites and immediately after 0.02 µm filtration for the Connecticut River mainstem sites; as such, the time between sample collection and Fe(II) measurement for the Connecticut River mainstem sites was the same as the amount of time between sample collection and 0.02 µm filtration (Table 1). Samples were stored un-acidified at 4 °C until measurement. Method details are described in Text S1. The measurement detection limit (Text S2, Table S1) was 0.006 mg L^{-1}.

Total iron was measured as total reducible iron using the Hach FerroVer method (Hach Method 8008) on either the Hach DR900 or the Hach FerroVer Pocket Colorimeter II within a median of 5 d after collection on samples stored un-acidified at 4 °C until measurement. Method details are described in Text S1. The measurement detection limit (Text S2, Table S1) was 0.010 mg L^{-1}. For a set of the samples collected at the Connecticut River at Thompsonville from August 2018 to October 2019, total dissolved

(< 0.22 µm) iron concentrations that were measured using the Hach FerroVer method were compared to total dissolved (< 0.45 µm) iron concentrations measured using inductively coupled plasma-atomic emission spectrometry (ICP-AES) (Fishman 1993; U.S. Geological Survey 2021). The two methods showed good agreement (Fig. S2), with < 0.22 µm concentrations using the Hach FerroVer method only 11% (0.012 mg L^{-1}) lower, on average, than the < 0.45 µm concentrations on ICP-AES. A small difference between the measurements is expected given the difference in filter pore size.

Fe(III) concentrations were calculated by subtracting the measured Fe(II) concentrations from the total Fe concentrations. It is important to note that here we report values below the measurement detection limits and that these values, therefore, will have higher uncertainty. While Fe(II) is rapidly oxidized to Fe(III) under the conditions typical of riverine surface waters and thus Fe(II) measurements are typically performed immediately after collection, our measurements of Fe(II) were performed within one to seven days of collection for the Connecticut River mainstem sites (Table 1), and thus likely represent the stable Fe(II) fraction, for example, complexed to DOM or sustained through DOM complexation reactions. The resulting Fe(III) concentrations calculated by difference are, therefore, more representative of the Fe(III) concentration at the time of spectrophotometric measurement, rather than the in-stream riverine Fe(III) concentrations, which are potentially lower. However, with respect to this analysis, it is the Fe(III) concentration at the time of measurement that is of interest, given the measurement of DOM spectrophotometric properties on samples refrigerated for short-term storage after collection is standard practice in many studies (Stedmon et al. 2003; Fellman et al. 2009; Spencer and Coble 2014; Mannino et al. 2019). For all measurements, the colloidal size fraction (0.02 to 0.22 µm) was calculated as the difference between the operationally dissolved (< 0.22 µm) and truly dissolved (< 0.02 µm) fractions (Gledhill and Buck 2012).

Dissolved organic matter chemistry and optical analysis

Dissolved organic carbon (DOC) concentrations for both size fractions were measured as non-purgeable organic carbon (NPOC) on a Shimadzu TOC-vCPH Analyzer (Shimadzu Corporation; Kyoto, Japan) within a median of 16 d after collection, and stored at 4 °C un-acidified before measurement. Standards and independent quality checks were measured for each run and were prepared according to Shimadzu protocol. Samples were acidified to 2% of 2 M HCl and sparged for five minutes as in Hosen et al. (2020). DOM ultraviolet–visible (UV–Vis) absorbance for both size fractions were performed on a Horiba Aqualog spectrometer (Horiba Scientific; Edison, NJ) within a median of 8 d after collection, and were stored at 4 °C without acidification until measurement, as both acidification and freeze/thaw have been shown to impact DOM absorption (Spencer et al. 2007). Samples were warmed to room temperature before measurement. UV–Vis absorbance was measured on a 1 cm pathlength from 239 to 800 nm at 3 nm increments with milli-Q water as a blank. Decadic UV–Vis absorption coefficients (a_{254} and a_{412}) were calculated by dividing the measured absorbance at the particular wavelength (λ) by the path length:

$$a_\lambda = \frac{A_\lambda}{l}$$

As in Poulin et al. (2014), measured a_λ can be corrected for Fe(III) by multiplying a wavelength-specific Fe(III) coefficient (a correction factor) by the Fe(III) concentration, and subtracting that from the measured decadic absorption at that wavelength (Text S3). The specific UV absorbance at 254 nm ($SUVA_{254}$) was calculated by dividing a_{254} by the DOC concentration, according to Weishaar et al. (2003). Fe(III)-corrected $SUVA_{254}$ was calculated by dividing the Fe(III)-corrected a_{254} by the DOC concentration.

Estimating Fe(III) contributions to UV absorption

In order to quantify the contributions of Fe(III) and DOC to the operationally dissolved UV–Vis absorbance (< 0.22 µm), coefficients for two different Fe(III) size fractions (truly dissolved, < 0.02 µm, and colloidal, 0.02–0.22 µm) and operationally dissolved DOC (< 0.22 µm) in the Connecticut River mainstem were derived using multiple linear regression and Type I ANOVA (Text S4). The same approach was also performed for Fe(III) and DOC in the operationally dissolved fraction (< 0.22 µm) only. In order to derive these coefficients, we assume that the only

source of UV-Vis absorption in the operationally dissolved fraction is either DOC or Fe(III), as is also done in Kritzberg and Ekström (2012) and in Xiao et al. (2013). The only other known biogeochemical constituent commonly present in natural waters that could potentially absorb in the < 0.22 µm fraction is nitrate (Weishaar et al. 2003), but dissolved nitrate concentrations in surface waters are too low to affect absorption at 254 nm (e.g., < 40 mg L^{-1}, Weishaar et al. 2003). Furthermore, Fe(II) has been shown to have a negligible impact on UV–Vis absorbance (Poulin et al. 2014).

To determine the impacts of failing to correct for Fe(III) absorption when measuring UV–Vis absorbance, we calculated the percent overestimation of a_{254} (which is equal to the overestimation of $SUVA_{254}$) and a_{412} due to Fe(III) absorption, by dividing the difference in uncorrected and Fe(III)-corrected a_{254} or a_{412} by the Fe(III)-corrected a_{254} or a_{412}. We use our operationally dissolved Fe(III) coefficient for 254 nm (see Eq. 2 in the "Results") and 412 nm (see Eq. S2) for the Connecticut River mainstem. We also compare results for a_{254} to the results using the Poulin et al. (2014) Fe(III) coefficient for 254 nm (6.53 L mg^{-1} m^{-1}) for both the Connecticut River mainstem sites and the tributary sites.

Results

Connecticut River mainstem

In the Connecticut River mainstem (Fig. 1a, Table 1), the percent difference in DOC between the operationally dissolved (< 0.22 µm) and truly dissolved (< 0.02 µm) fractions averaged 3.4 ± 3.8% (Fig. 2, Table 3), and the average absolute difference was 0.1 ± 0.1 mg L^{-1}. This was statistically different using a paired t-test ($p < 0.001$). The difference in DOC concentrations between the two fractions did not exceed 0.4 mg L^{-1}. Mainstem average operationally dissolved Fe(III) was around five times greater than truly dissolved Fe(III) (Table 3). Thus, 78.5 ± 20.9%, or 0.063 ± 0.039 mg L^{-1}, of Fe(III) was removed from the operationally dissolved fraction with subsequent 0.02 µm filtration (i.e., was colloidal) (Fig. 2, Table 3). The difference in Fe(III) between the operationally and truly dissolved size

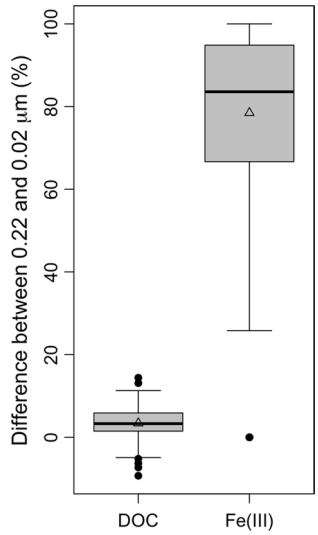

Fig. 2 Percent difference in DOC and Fe(III) concentration between the operationally dissolved (< 0.22 µm) and truly dissolved (< 0.02 µm) size fractions in the Connecticut River mainstem. Line represents the median and open triangle represents the mean

fractions was statistically significant using a paired t-test ($p < 0.001$).

The average operationally dissolved a_{254} was 11.5 ± 4.0 m^{-1} and truly dissolved a_{254} was 10.1 ± 3.6 m^{-1} (Table 3). This results in an a_{254} difference of 12.0 ± 5.5% between the operationally and truly dissolved fractions, which was nearly four times greater than the difference in DOC between the two fractions (Table 3). Similarly, there was a 21.2 ± 11.1% (0.2 ± 0.1 m^{-1}) difference in a_{412} between the two fractions (Table 3), which is roughly seven times greater than the difference in DOC. $SUVA_{254}$ averaged 3.5 ± 0.4 L mg^{-1} m^{-1} and 3.2 ± 0.3 L mg^{-1} m^{-1} in the operationally and truly dissolved fractions, respectively (Table 3), which is on average 9.1 ± 6.3%, or nearly three times, the difference in DOC between the two fractions (Table 3). For a_{254}, a_{412}, and $SUVA_{254}$, the difference between the operationally and truly dissolved fractions was significant using a paired t-test ($p < 0.001$).

Connecticut River tributary sites

The average operationally dissolved DOC concentration in the seven tributary sites (Fig. 1b, Table 2) was 2.5 ± 0.8 mg L^{-1}. The average operationally

Table 3 Average concentrations of DOC and Fe(III) and a_{254}, a_{412}, and $SUVA_{254}$ for each size fraction (operationally dissolved, < 0.22 and truly dissolved, < 0.02 µm) and the absolute and percent difference between the size fractions (equivalent to colloidal) in the Connecticut River mainstem

	< 0.22	< 0.02	0.22–0.02[b]	0.22–0.02 (%)
DOC (mg L^{-1})	3.2 (0.8)[a]	3.1 (0.9)	0.1 (0.1)	3.4 (3.8)
Fe(III) (mg L^{-1})	0.079 (0.046)	0.015 (0.015)	0.063 (0.039)	78.5 (20.9)
a_{254} (m^{-1})	11.5 (4.0)	10.1 (3.6)	1.4 (0.7)	12.0 (5.5)
a_{412} (m^{-1})	1.0 (0.4)	0.8 (0.4)	0.2 (0.1)	21.2 (11.1)
$SUVA_{254}$ (L mg^{-1} m^{-1})	3.5 (0.4)	3.2 (0.3)	0.3 (0.2)[c]	9.1 (6.3)[c]

[a]Standard deviation listed in parentheses

[b]Calculated by difference. This difference is also equal to the colloidal size fraction

[c]Difference calculated by subtracting the operationally and truly dissolved $SUVA_{254}$, not by dividing colloidal a_{254} and colloidal DOC

dissolved Fe(III) concentration was 0.167 ± 0.098 mg L^{-1}. Operationally dissolved a_{254} and a_{412} were 9.0 ± 1.8 m^{-1} and 0.9 ± 0.2 m^{-1}, respectively. $SUVA_{254}$ in the operationally dissolved fraction averaged 3.8 ± 1.0 L mg^{-1} m^{-1}.

Discussion

Difference between size fractions

Size fractionation can be a useful tool to isolate the impacts of Fe(III) on UV–Vis absorbance. While size fractionation is commonly used to evaluate interactions between trace metals and DOM (Stolpe et al. 2010, 2012; Zhou et al. 2016; Wang et al. 2017), little attention has been given to using it as a method to isolate the impacts of absorbing colloidal material, like iron, present in operationally dissolved filtrate. In the Connecticut River mainstem, there was a negligible difference in DOC between the operationally dissolved (< 0.22 µm) and truly dissolved (< 0.02 µm) fractions, demonstrating that nearly all the DOM is truly dissolved (Table 3). Additionally, plotting DOC in the operationally versus truly dissolved fraction resulted in a strong positive relationship falling approximately on the 1:1 line (Fig. 3a). This indicates little presence of colloidal (0.02–0.22 µm) DOM in the Connecticut River mainstem.

While there was no difference in DOC between the operationally and truly dissolved fractions in our system, there was a difference in UV–Vis absorbance. a_{254} and a_{412} were four and six times greater, respectively, in the operationally dissolved fraction compared to the truly dissolved fraction (Table 3), suggesting the presence of absorbing colloidal material. Additionally, a_{254}, a_{412}, and $SUVA_{254}$ deviated from the 1:1 line, with greater absorbance in the operationally dissolved fraction (Fig. 3b-d). While higher molecular weight DOM has been shown to be more highly absorbing (Chin et al. 1994), colloidal DOC concentrations were extremely low in the Connecticut River samples (0.1 mg L^{-1}, on average, maximum of 0.4 mg L^{-1}) and were not correlated to colloidal a_{254} or a_{412} (Fig. S3a-b). This demonstrates that the greater UV–Vis absorbance in the operationally dissolved fraction compared to the truly dissolved fraction is due to the presence of absorbing colloidal material that is not DOM.

Ferric iron in the colloidal fraction contributes to the greater UV–Vis absorbance in the operationally dissolved fraction compared to the truly dissolved fraction. For the Connecticut River mainstem, Fe(III) concentrations in the operationally dissolved fraction were five times greater than in the truly dissolved fraction; in fact, most Fe(III) was removed following 0.02 µm filtration, and thus Fe(III) was predominantly colloidal (Fig. 2, Table 3). Furthermore, while there was no relationship between colloidal a_{254} or a_{412} and colloidal DOC (Fig. S3a-b), there was a positive correlation between colloidal a_{254} or a_{412} and colloidal Fe(III) (Fig. S3c-d). This suggests that colloidal Fe(III) is the absorbing colloidal material that contributed to the greater UV–Vis absorbance in the operationally dissolved fraction compared to the truly dissolved fraction.

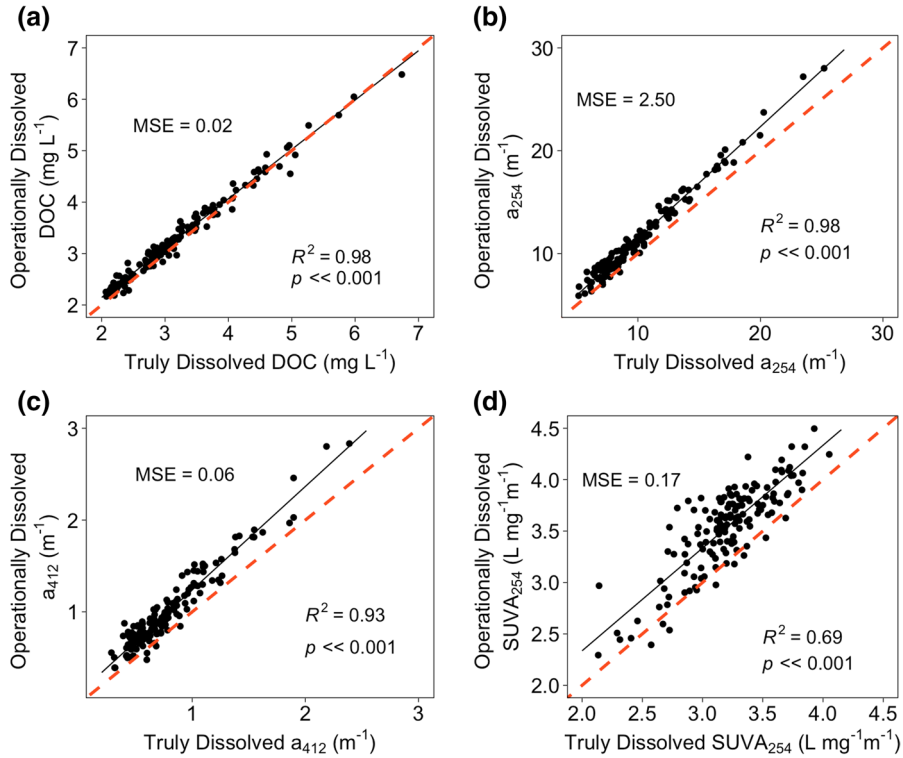

Fig. 3 Operationally dissolved (< 0.22 µm) versus truly dissolved (< 0.02 µm) fractions for **a** DOC, **b** a_{254}, **c** a_{412}, and **d** $SUVA_{254}$ in the Connecticut River mainstem. The orange dashed line represents the 1:1 line. The mean square error (MSE) displayed is the mean of the square of the difference between the operationally and truly dissolved fractions

Variable Fe(III) contributions to UV–Vis absorbance

The two Fe(III) size fractions contribute to UV–Vis absorbance differently. Multiple linear regression determined the contributions of operationally dissolved DOC (< 0.22 µm), colloidal Fe(III) (0.02–0.22 µm), and truly dissolved Fe(III) (< 0.02 µm) on operationally dissolved a_{254} (< 0.22 µm) for the Connecticut River mainstem:

$$a_{254<0.22,measured} = 3.8(\pm0.1)DOC_{<0.22} + 12.7(\pm2.2)Fe^{3+}_{0.02-0.22} + 44.2(\pm6.4)Fe^{3+}_{<0.02} - 2.3(\pm0.3) \quad (1)$$

DOC and both Fe(III) size fractions are in mg L^{-1} and a_{254} is in m^{-1}. Coefficients for Fe(III) and DOC (L mg^{-1} m^{-1}) can be used to correct a_{254} measurements for Fe(III) contributions, as in Poulin et al. (2014) (Text S3). Standard error for each coefficient and the intercept is presented in parentheses following the coefficient or intercept. The multiple linear regression had an adjusted R^2 of 0.94 ($p < 0.001$) and each individual coefficient (i.e., DOC < 0.22 µm and both Fe(III) fraction sizes) was significant using Type I ANOVA ($p < 0.001$). The tenfold cross-validation produced an R^2 of 0.94 and a root mean square error (RMSE) of 0.98. The same approach in Eq. 1 was used for a_{412}, producing similar results (Equation S1). For a_{254}, the coefficient for colloidal Fe(III) was more than three times greater than the coefficient for operationally dissolved DOC. While the concentration of Fe(III) in the truly dissolved fraction was low, the coefficient for truly dissolved Fe(III) was four times greater than the coefficient for colloidal Fe(III), demonstrating greater absorption per unit concentration for truly dissolved Fe(III) than colloidal Fe(III).

The different coefficients for Fe(III) by size fraction demonstrate that Fe(III) coefficients may vary by speciation or source. This idea is consistent with other studies that report different absorption spectra for different species of Fe(III) (Sherman and Waite 1985; Stefánsson 2007; Loures et al. 2013) or for Fe(III) that is produced by Fe(II) oxidation (Stefánsson 2007; Poulin et al. 2014). The "soluble" or truly dissolved Fe(III) pool, defined as Fe(III) smaller than 0.02 µm

(Gledhill and Buck 2012), is likely mostly composed of a DOM-bound ferric iron pool (Stolpe et al. 2012; Joung and Shiller 2016) whereas the colloidal iron pool, from 0.02 to 0.22 µm, is predominantly inorganic iron, such as hydrous ferric oxides (Stolpe et al. 2012). Thus, the species and/or size class of iron is important in determining the contribution of Fe(III) to DOM absorption, and this contribution will likely change across systems, as the distribution of Fe(III) between size fractions varies.

We also derived a single operationally dissolved Fe(III) coefficient for operationally dissolved a_{254}, as in other studies:

$$a_{254<0.22,measured} = 4.1(\pm0.1)DOC_{<0.22} + 16.8(\pm2.2)Fe^{3+}_{<0.22} - 2.8(\pm0.3) \quad (2)$$

The multiple linear regression for the operationally dissolved Fe(III) fraction had an adjusted R^2 of 0.93 ($p < 0.001$), and both coefficients (i.e., operationally dissolved Fe(III) and DOC) were significant using Type I ANOVA ($p < 0.001$). The tenfold cross-validation produced an R^2 of 0.93 and an RMSE of 1.03. The coefficient for operationally dissolved Fe(III) was four times greater than the coefficient for DOC (Eq. 2). Equation S2 describes the operationally dissolved Fe(III) coefficient for a_{412}, which showed a six times greater absorption by Fe(III) per unit concentration compared to DOC.

Fe(III) contributions to UV absorbance in our system are greater than previously reported estimates. While the linear increase in UV absorbance with increasing Fe(III) concentration observed in this study (Fig. S3c-d) is consistent with past findings (Weishaar et al. 2003; Xiao et al. 2013; Poulin et al. 2014; Brezonik et al. 2019), the Fe(III) coefficients derived in Eqs. 1 and 2 are greater than some previously reported estimates (Table S2). However, Fe(III) coefficients for various wavelengths and the methods used to determine them are highly variable across studies (Table S2), and only a few examine Fe(III) contributions to absorbance using natural water samples. Interestingly, our estimate for the operationally dissolved Fe(III) coefficient at 412 nm is similar to existing estimates for DOM-complexed Fe(III) at 410 nm (Table S2, Eq. S2 compared to Xiao et al. 2013). Along with the large range in reported Fe(III) coefficients, this suggests that using a single wavelength-specific Fe(III) coefficient as a correction factor for all systems may under- or overestimate the contribution of Fe(III) to UV–Vis absorbance.

Evaluating the effectiveness of Fe(III) correction

Given the lack of colloidal DOC in our system, we were able to use size fractionation to evaluate the effectiveness of Fe(III) coefficients (i.e., correction factors) in correcting UV–Vis absorbance measurements for Fe(III) by comparing the operationally versus truly dissolved fractions before and after Fe(III) correction (Fig. 4, Fig. S4). We evaluate the effectiveness of these correction factors using 1:1 lines and the mean square error (MSE).

The Poulin et al. (2014) Fe(III) coefficient underestimates the contributions of Fe(III) to a_{254} in the Connecticut River mainstem, while the Fe(III) coefficients derived in Eqs. 1 and 2 more sufficiently correct for Fe(III) interference. Applying Fe(III) corrections to both operationally and truly dissolved a_{254} using either the two Fe(III) size fraction coefficients (Eq. 1) or the operationally dissolved Fe(III) coefficient (Eq. 2) resulted in operationally and truly dissolved a_{254} and $SUVA_{254}$ falling closer to the 1:1 line and having a lower MSE than for uncorrected a_{254} and $SUVA_{254}$ (Fig. 4a, b, d, e). Results were similar for a_{412} (Fig. S4). The corrections for a_{254}, and subsequently $SUVA_{254}$, had a better fit (closer to the 1:1 line and lower MSE) than the Poulin et al. (2014) correction, for which there was little improvement compared to before correction (Fig. 4c, f). Fe(III)-corrected $SUVA_{254}$ operationally versus truly dissolved plots using Eqs. 1 or 2 (Fig. 4d-e) had less scatter (higher R^2) than both uncorrected $SUVA_{254}$ (Fig. 3d) and the Poulin et al. (2014) corrected $SUVA_{254}$ (Fig. 4f). This evidence suggests that a single, wavelength-specific Fe(III) correction factor for all systems may not sufficiently correct measurements of DOM UV–Vis absorbance for Fe(III) in all natural waters.

Applying the Fe(III) coefficient from Eq. 2 from the mainstem sites to the tributary sites results in a large over-correction of $SUVA_{254}$. For example, the Fe(III)-corrected $SUVA_{254}$ for Bunnell Brook using the Eq. 2 coefficient was 0.6 L mg^{-1} m^{-1} compared

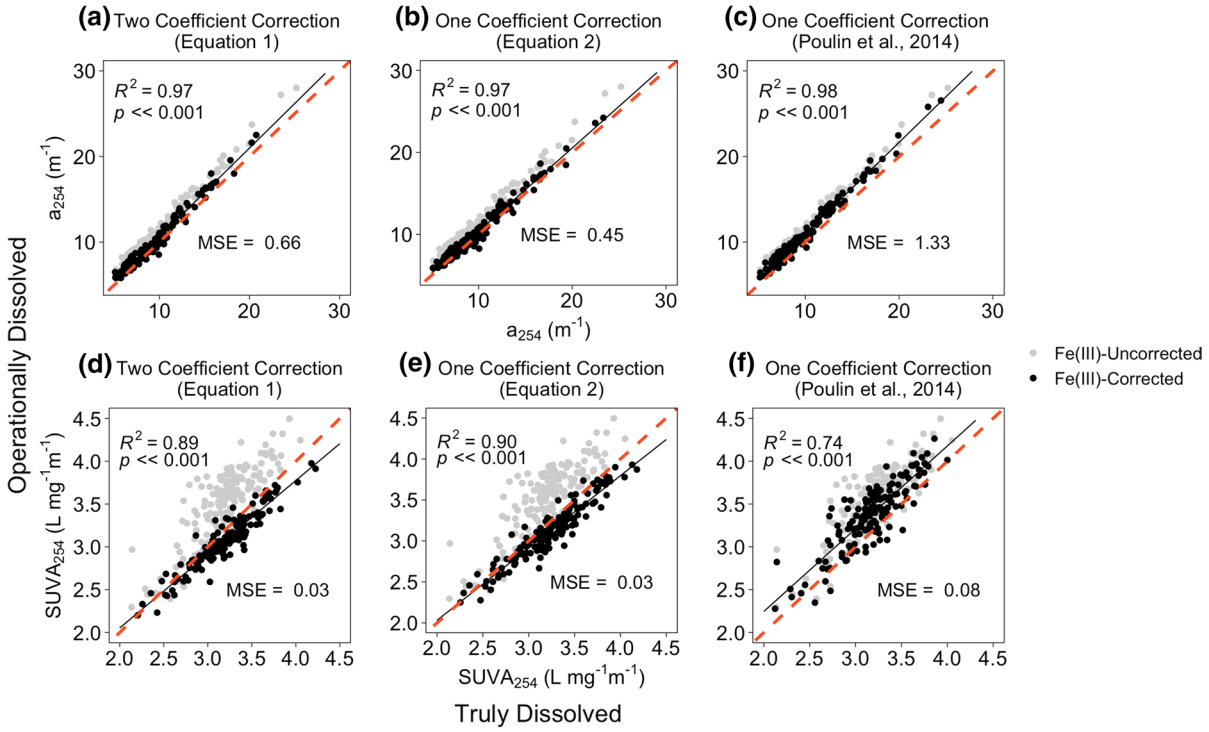

Fig. 4 Operationally dissolved (<0.22 µm) versus truly dissolved (<0.02 µm) Fe(III)-corrected **a**–**c** a_{254} and **d**–**f** $SUVA_{254}$. Fe(III) correction was performed on both the operationally and truly dissolved fractions using either the **a**, **d** colloidal and truly dissolved Fe(III) coefficients calculated in this study (Eq. 1), **b**, **e** the operationally dissolved Fe(III) coefficient calculated in this study (Eq. 2), or **c**, **f** the operationally dissolved Poulin et al. (2014) Fe(III) coefficient. Light grey points are the Fe(III)-uncorrected **a**–**c** a_{254} and **d**–**f** $SUVA_{254}$ in the operationally versus truly dissolved fractions, for reference. The orange, dashed line represents the 1:1 line. Data are for the Connecticut River mainstem only. The mean square error (MSE) displayed is the mean of the square of the difference between the Fe(III)-corrected operationally and truly dissolved fractions

to 5.8 L mg^{-1} m^{-1} uncorrected. Thus, even our correction factors developed at a river mainstem do not hold for a tributary site only 37 km away from the closest Connecticut River mainstem site. Correction of UV–Vis absorbance for Fe(III) may also be more challenging in smaller streams because increased flashiness results in much greater variability in DOC and Fe(III) concentrations and DOM composition.

Fe(III)/DOC and UV–Vis overestimation

The percent overestimation of a_{254} and a_{412} is approximately proportional to the ratio of the concentration of Fe(III) to the concentration of DOC. At wavelength λ, the percent overestimation of a_λ can be simplified to:

$$a_\lambda overestimation(\%) = \frac{c.f. \times \mathrm{Fe(III)}}{a_{\lambda \mathrm{Fe(III)} corrected}} \quad (3)$$

where c.f. is the correction factor (Fe(III) coefficient) used. The concentration of DOC is highly correlated to UV–Vis absorbance ($R^2 = 0.91$ and 0.83 for Fe(III)-corrected a_{254} and a_{412}, respectively, $p < 0.001$), and so Eq. 3 can be substituted by the ratio of Fe(III)/DOC (Fig. S5 and S6). This explains why the contribution of Fe(III) to UV–Vis absorbance is shown to be correlated to the Fe(III)/DOC ratio (Xiao et al. 2013, 2015; Brezonik et al. 2019). As such, the Fe(III)/DOC ratio can be used to determine the importance of iron correction in a particular system (Fig. S5 and S6). Furthermore, contributions of Fe(III) to absorbance can be high even when Fe(III) concentrations are low, if DOC concentrations are low.

The ratio of Fe(III) to DOC

Factors such as stream size, discharge (Gaffney et al. 2008; Raymond and Saiers 2010; Xiao et al. 2015), and land use (Xiao et al. 2015) drive Fe(III) and DOC concentrations, sometimes separately, impacting the Fe(III)/DOC ratio. This decoupling may create systematic biases of UV–Vis absorbance and $SUVA_{254}$. Below we demonstrate the potential pitfalls of Fe(III) biases on DOM composition and amount.

Stream size

Fe(III):DOC and, therefore, UV–Vis overestimation, may vary by stream size. Lower operationally dissolved Fe(III) concentrations have been observed with increasing stream order (Neubauer et al. 2013), whereas DOC concentrations are less consistently variable with increasing stream size (Table S3, Hosen et al. 2020). Thus, Fe(III):DOC is expected to decrease with increasing stream order. This was captured in our system. Both the Fe(III):DOC ratio and the overestimation of a_{254} or $SUVA_{254}$ were, on average, almost four times greater in the seven tributary sites sampled synoptically during the summer of 2019 than in the Connecticut River mainstem, when using the same Fe(III) coefficient to correct for Fe(III) in both systems (Table S4). a_{254} and $SUVA_{254}$ overestimation in the Connecticut River mainstem had a median of $14 \pm 7\%$ and a maximum overestimation of 31% using the Fe(III) coefficient from Eq. 2, and $5 \pm 2\%$ using the more conservative Poulin et al. (2014) coefficient (Table S4). For the seven smaller tributaries in the Connecticut River watershed that were sampled in the summer 2019, the overestimation of a_{254} and $SUVA_{254}$ was greater and had a larger range compared to the Connecticut River mainstem (median $= 12 \pm 17\%$ using the Poulin et al., 2014 coefficient, Table S4). The greatest overestimation was 53% at Bunnell Brook, for which an Fe(III) concentration of 0.341 mg L^{-1} and DOC concentration of 1.1 mg L^{-1} (Table S3) led to $SUVA_{254}$ being calculated as 5.8 L mg^{-1} m^{-1} instead of the Fe(III)-corrected value of 3.8 L mg^{-1} m^{-1}. Of the seven Connecticut River watershed sites sampled during the summer 2019, the Connecticut River mainstem at Thompsonville had the lowest overestimation. Therefore, Fe(III) contributions to absorbance may be more important in smaller tributaries than large rivers.

Land use

Land use is correlated to the Fe(III):DOC ratio, and therefore, UV–Vis overestimation. Land use has been shown to affect aquatic DOM composition (Lambert et al. 2017), DOC concentrations (Cronan et al. 1999), and iron concentrations (Neubauer et al. 2013; Taka et al. 2016). If land use impacts DOC and iron concentrations differently (i.e., if they are decoupled), then the Fe(III):DOC ratio might change with land use. In the Connecticut River tributary sites, we found a decoupling of Fe(III) and DOC concentrations, resulting in land-use driven trends in Fe(III):DOC. For the seven tributary sites sampled during the summer 2019, there was a strong positive correlation between the Fe(III):DOC ratio and the percent land cover as agriculture ($R^2 = 0.75$, $p = 0.011$), and therefore, between the percent a_{254} or $SUVA_{254}$ overestimation and percent land cover as agriculture ($R^2 = 0.75$, $p = 0.012$), when using the Poulin et al. (2014) Fe(III) coefficient. This was similarly observed in Xiao et al. (2015), in which catchments with a greater proportion of agriculture resulted in a greater riverine concentration of Fe(III) relative to DOC. Percent agricultural land was also weakly negatively correlated with percent forested land ($R^2 = 0.34$, $p = 0.17$), and thus Fe(III):DOC and a_{254} and $SUVA_{254}$ overestimation decreased with increasing forest cover as well ($R^2 = 0.58$, $p = 0.045$). Failing to address or correct for Fe(III) across systems with varying land use could systematically overestimate DOM quantity or quality due to the differing interference of Fe(III).

Samples from the Connecticut River watershed demonstrate the potential for misinterpreting DOM quality across a land-use gradient. Iron interference was so high in sites with a large percentage of agriculture (and low percentage of forested area) that DOM aromaticity (determined by Fe(III)-uncorrected $SUVA_{254}$) seemed to be mainly driven by percent forested land or percent agriculture (Fig. 5a, c, $R^2 > 0.60$ and $p < 0.05$ for both). Correcting for Fe(III) using the Poulin et al. (2014) Fe(III) coefficient resulted in the relationship between $SUVA_{254}$ and percent forest and percent agriculture weakening (Fig. 5a, c, $R^2 < 0.40$ and $p > 0.1$ for both), and the relationship with percent wetland becoming stronger (Fig. 5b, R^2 increased from 0.26 to 0.49 and p decreased from 0.24 to 0.08). This relationship with Fe(III)-corrected

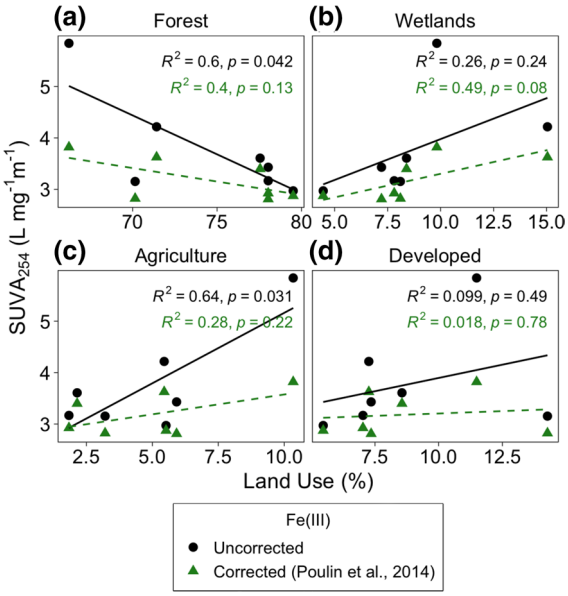

Fig. 5 Fe(III)-uncorrected (black circles) and Fe(III)-corrected (green triangles) $SUVA_{254}$ using the Fe(III) coefficient from Poulin et al. (2014) compared to percent **a** forest, **b** wetland, **c** agriculture, and **d** developed land use in the watersheds for the seven sites sampled in the summer 2019

$SUVA_{254}$ and percent wetland (originally biased by trends between Fe(III) and agriculture) is in line with studies that have shown that DOM aromaticity increased with percent wetland in a watershed and decreased with percent agriculture (Wilson and Xenopoulos 2008). These results demonstrate that by failing to correct for Fe(III) contributions to UV–Vis absorbance, observed trends in UV–Vis estimated DOM aromaticity and land use were actually dominated by relationships between Fe(III):DOC ratios and land use.

Seasonality and discharge

The seasonal variability in Fe(III):DOC observed here cautions against the presentation of seasonal DOM results based on UV–Vis absorbance without also presenting Fe(III) concentrations. This is particularly important given the same drivers of DOM composition and amount (e.g., DOM source) impact the Fe(III):DOC ratio. In the winter and at low flow, highly absorbing and aromatic (i.e., high $SUVA_{254}$) allochthonous DOM in the Connecticut River mainstem is low (Shultz et al. 2018; Hosen et al. 2020), resulting in both low DOC concentrations (low a_{254} and low a_{412}) and expected lower $SUVA_{254}$. In our study, the Fe(III):DOC ratio was significantly greater in the winter than in the other three seasons ($p < 0.05$). Additionally, the Fe(III):DOC ratio and therefore a_{254}, a_{412}, and $SUVA_{254}$ overestimation was negatively correlated to discharge in the spring (Fig. 6a, $R^2 = 0.85$, $p < 0.001$). This could result in the weakening of seasonal and discharge-driven trends in DOM composition and amount (i.e., overestimating low $SUVA_{254}$ and low CDOM concentrations in the winter and at low flow in the spring). This is particularly problematic in systems that show a large variability in Fe(III) and/or DOC concentration seasonally or with discharge (e.g., small tributaries).

The source of iron also dictates the relationship between Fe(III) concentration and discharge. For example, both Stolpe et al. (2012) and Ingri et al. (2006) showed that two dominant types of Fe in boreal river systems, Fe(III)-oxyhydroxides and Fe complexed to DOM, varied with river discharge. If Fe(III) absorption is indeed speciation- or size-dependent as we suggest, the absorption of Fe(III) and, therefore, the total contribution of Fe(III) to UV–Vis absorbance, may also vary with discharge.

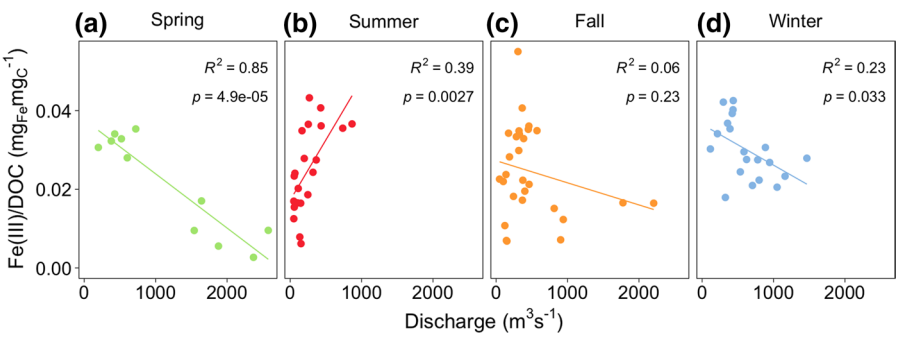

Fig. 6 Trends in operationally dissolved (< 0.22 µm) Fe(III)/DOC versus discharge for the **a** spring, **b** summer, **c** fall, and **d** winter in the Connecticut River mainstem at Thompsonville, Middle Haddam, and Northfield

Thus, seasonal differences in both the discharge-driven controls on Fe(III) speciation and DOC coupling impact the importance of discharge in driving UV–Vis absorbance and overestimation. Consideration of Fe(III) is, therefore, imperative for studies of seasonal DOM composition and concentration.

Routine measurement of Fe(III) in tandem with CDOM optics

Using sequential filtration to derive size-specific Fe(III) coefficients provides challenges that make it difficult to recommend routinely adopting for studies employing CDOM UV–Vis measurements. Firstly, ultrafiltration through 0.02 µm is time and cost-intensive. Furthermore, while sequential filtration through 0.02 µm does, to some extent, separate two distinct pools of iron with different absorption properties (e.g., organically-bound Fe(III) and inorganic Fe(III)), it does not do so completely. Thus the contributions of different Fe(III) species to absorbance in the operationally dissolved fraction likely also vary from system to system; for example, the Fe(III) coefficients derived in Eqs. 1 and 2 for the Connecticut River mainstem could not be applied to the tributary sites. However, correcting a_{254} or a_{412} for Fe(III) using the system-specific coefficient for operationally dissolved Fe(III) in Eq. 2 corrected just as well, if not better, than the two Fe(III) coefficients in Eq. 1, suggesting that it is less important to use separate Fe(III) size fractions to correct for Fe(III), as long as the coefficients (i.e., correction factors) are system specific. Thus, including dissolved Fe(III) measurements in studies that measure DOM UV–Vis absorption is paramount.

Total Fe and Fe(II) concentrations can be easily measured using a field colorimeter or spectrophotometer. Following the methods here (e.g., Hach Method 8146 and Method 8008), total iron and Fe(II) can be measured with a field colorimeter. Alternatively, total Fe and Fe(II) concentrations can be measured on the same spectrophotometer and on the same filtered sample for which a_{254} and a_{412} is measured. For example, the filtered sample blank absorption at the same wavelength that the 1,10-phenanthroline complex absorbs at (~508 nm) is typically already measured when CDOM absorbance is measured and can be subtracted from the absorbance measurement at the same wavelength after adding 1,10-phenanthroline for Fe(II) or the FerroVer reagent for total Fe. As such, ferric iron measurements can be easily conducted alongside CDOM UV–Vis absorbance measurements. Thus, inclusion of Fe(III) data should become standard practice when presenting CDOM UV–Vis absorbance.

Conclusions

This study provides an in-depth analysis testing existing Fe(III) coefficients (i.e., correction factors) used to correct for Fe(III) contributions to UV–Vis absorbance in natural water samples. We have shown that Fe(III) absorption at 254 nm and 412 nm results in significantly higher a_{254}, a_{412}, and $SUVA_{254}$ in operationally dissolved (< 0.22 µm) natural water samples compared to when the majority of Fe(III), but not DOC, is removed by subsequent 0.02 µm filtration (truly dissolved fraction). While current Fe(III) coefficients used for Fe(III) correction apply broadly to the operationally dissolved fraction (e.g., Poulin et al. 2014), we demonstrated that colloidal (0.02–0.22 µm) and truly dissolved Fe(III) impacted UV absorbance differently, with truly dissolved Fe(III) having a greater contribution to absorbance than colloidal Fe(III) per unit concentration. This suggests variability in Fe(III) absorption by speciation or source and complicates the use of single, wavelength-specific Fe(III) coefficients (i.e., correction factors), proposed for correction of UV–Vis absorbance measurements. This complication was illustrated by the fact that existing coefficients commonly used for Fe(III) correction (Poulin et al. 2014) did not entirely account for Fe(III) contributions to measured a_{254} and $SUVA_{254}$ in our system. Additional work is needed to characterize and evaluate the variability in Fe(III) UV–Vis absorption by size, speciation, and source in natural waters. Collectively, the evidence presented here argues that measurement of Fe(III) in studies employing DOM optics should become routine, even in systems where high Fe(III) concentrations are not to be expected. Failing to do so may lead to significant overestimation of DOM optical parameters such as a_{254}, a_{412}, and $SUVA_{254}$, and even more troubling, seasonal, discharge-driven, or land-use trends in DOM quality or quantity being unknowingly overshadowed by trends in Fe(III).

Acknowledgements All measurements were performed at Yale University, School of the Environment. A special thanks to Jonas Karosas for help troubleshooting the Shimadzu TOC-V. We also thank Bea Pickett for assistance with lab work, Guy Holzer and Brittney Izbicki for coordinating and conducting sampling at Northfield, Thompsonville, and Middle Haddam, bi-weekly, the Connecticut River Museum and CT DEEP for site access, and Taylor Maavara, Kristen Jabanoski, and Itai Boneh for assistance sampling the CT River watershed sites during the summer 2019. We thank Jennifer Tank and two anonymous reviewers for their constructive comments that helped improve the content and clarity of this manuscript.

Funding This work was supported by the Yale Institute for Biospheric Studies and the National Science Foundation (NSF) Grant DEB-1840243.

Data availability The data are openly available in an online repository (https://doi.org/10.5281/zenodo.6092729).

Code availability Not applicable.

Declarations

Conflict of interest The authors have no conflicts of interest or competing interests to declare that are relevant to the content of this article.

Open Access This article is licensed under a Creative Commons Attribution 4.0 International License, which permits use, sharing, adaptation, distribution and reproduction in any medium or format, as long as you give appropriate credit to the original author(s) and the source, provide a link to the Creative Commons licence, and indicate if changes were made. The images or other third party material in this article are included in the article's Creative Commons licence, unless indicated otherwise in a credit line to the material. If material is not included in the article's Creative Commons licence and your intended use is not permitted by statutory regulation or exceeds the permitted use, you will need to obtain permission directly from the copyright holder. To view a copy of this licence, visit http://creativecommons.org/licenses/by/4.0/.

References

Alcântara E, Bernardo N, Rodrigues T, Watanabe F (2017) Modeling the spatio-temporal dissolved organic carbon concentration in Barra Bonita reservoir using OLI/Landsat-8 images. Model Earth Syst Environ 3:1–6. https://doi.org/10.1007/s40808-017-0275-2

Asmala E, Stedmon CA, Thomas DN (2012) Linking CDOM spectral absorption to dissolved organic carbon concentrations and loadings in boreal estuaries. Estuar Coast Shelf Sci 111:107–117. https://doi.org/10.1016/j.ecss.2012.06.015

Baken S, Degryse F, Verheyen L et al (2011) Metal complexation properties of freshwater dissolved organic matter are explained by its aromaticity and by anthropogenic ligands. Environ Sci Technol 45:2584–2590. https://doi.org/10.1021/es103532a

Benner R (2003) 5. Molecular indicators of the bioavailability of dissolved organic matter. In: Findlay SEG, Sinsabaugh RLBT (eds) Aquatic ecology. Academic Press, Burlington, pp 121–137

Brezonik PL, Finlay JC, Griffin CG et al (2019) Iron influence on dissolved color in lakes of the Upper Great Lakes States. PLoS ONE 14:1–20

Bricaud A, Morel A, Prieur L (1981) Absorption by dissolved organic matter to the sea (yellow substance) in the UV and visible domains. Limnol Oceanogr 26:43–53

Cao F, Tzortziou M, Hu C et al (2018) Remote sensing retrievals of colored dissolved organic matter and dissolved organic carbon dynamics in North American estuaries and their margins. Remote Sens Environ 205:151–165. https://doi.org/10.1016/j.rse.2017.11.014

Chin YP, Alken G, O'Loughlin E (1994) Molecular weight, polydispersity, and spectroscopic properties of aquatic humic substances. Environ Sci Technol 28:1853–1858. https://doi.org/10.1021/es00060a015

Cronan CS, Piampiano JT, Patterson HH (1999) Influence of land use and hydrology on exports of carbon and nitrogen in a Maine river basin. J Environ Qual 28:953–961. https://doi.org/10.2134/jeq1999.00472425002800030028x

Fellman JB, Hood E, Edwards RT, Amore DVD (2009) Changes in the concentration, biodegradability, and fluorescent properties of dissolved organic matter during stormflows in coastal temperate watersheds. J Geophys Res 114:1–14. https://doi.org/10.1029/2008JG000790

Fichot CG, Benner R (2011) A novel method to estimate DOC concentrations from CDOM absorption coefficients in coastal waters. Geophys Res Lett 38:1–5. https://doi.org/10.1029/2010GL046152

Fishman MJ (1993) Methods of analysis by the U.S. Geological Survey National Water Quality Laboratory -- Determination of Inorganic and Organic Constituents in Water and Fluvial Sediments. Denver, CO

Gaffney JW, White KN, Boult S (2008) Oxidation state and size of Fe controlled by organic matter in natural waters. Environ Sci Technol 42:3575–3581. https://doi.org/10.1021/es702880a

Gledhill M, Buck KN (2012) The organic complexation of iron in the marine environment: a review. Front Microbiol 3:1–17. https://doi.org/10.3389/fmicb.2012.00069

Helms JR, Stubbins A, Ritchie JD et al (2008) Absorption spectral slopes and slope ratios as indicators of molecular weight, source, and photobleaching of chromophoric dissolved organic matter. Limnol Oceanogr 53:955–969. https://doi.org/10.4319/lo.2008.53.3.0955

Hernes PJ, Benner R (2003) Photochemical and microbial degradation of dissolved lignin phenols: Implications for the fate of terrigenous dissolved organic matter in marine environments. J Geophys Res 108:3291. https://doi.org/10.1029/2002JC001421

Hosen JD, Aho KS, Fair JH et al (2020) Source switching maintains dissolved organic matter chemostasis across discharge levels in a large temperate river network. Ecosystems. https://doi.org/10.1007/s10021-020-00514-7

Ingri J, Malinovsky D, Rodushkin I et al (2006) Iron isotope fractionation in river colloidal matter. Earth Planet Sci Lett 245:792–798. https://doi.org/10.1016/j.epsl.2006.03.031

Ingri J, Conrad S, Lidman F et al (2018) Iron isotope pathways in the boreal landscape: Role of the riparian zone. Geochim Cosmochim Acta 239:49–60. https://doi.org/10.1016/j.gca.2018.07.030

Joung D, Shiller AM (2016) Temporal and spatial variations of dissolved and colloidal trace elements in Louisiana Shelf waters. Mar Chem 181:25–43. https://doi.org/10.1016/j.marchem.2016.03.003

Kikuchi T, Fujii M, Terao K et al (2017) Correlations between aromaticity of dissolved organic matter and trace metal concentrations in natural and effluent waters: a case study in the Sagami River Basin, Japan. Sci Total Environ 576:36–45. https://doi.org/10.1016/j.scitotenv.2016.10.068

Kitis M, Karanfil T, Wigton A, Kilduff JE (2002) Probing reactivity of dissolved organic matter for disinfection by-product formation using XAD-8 resin adsorption and ultrafiltration fractionation. Water Res 36:3834–3848

Kritzberg ES, Ekström SM (2012) Increasing iron concentrations in surface waters—a factor behind brownification? Biogeosciences 9:1465–1478. https://doi.org/10.5194/bg-9-1465-2012

Lambert T, Bouillon S, Darchambeau F et al (2017) Effects of human land use on the terrestrial and aquatic sources of fluvial organic matter in a temperate river basin (The Meuse River, Belgium). Biogeochemistry 136:191–211. https://doi.org/10.1007/s10533-017-0387-9

Loures CCA, Alcântara MAK, Filho HJI et al (2013) Advanced oxidative degradation processes: fundamentals and applications. Int Rev Chem Eng 5:102. https://doi.org/10.15866/ireche.v5i2.6909

Maloney KO, Morris DP, Moses CO, Osburn CL (2005) The role of iron and dissolved organic carbon in the absorption of ultraviolet radiation in humic lake water. Biogeochemistry. https://doi.org/10.1007/s10533-005-1675-3

Mannino A, Novak MG, Hooker SB et al (2014) Algorithm development and validation of CDOM properties for estuarine and continental shelf waters along the northeastern U.S. coast. Remote Sens Environ 152:576–602. https://doi.org/10.1016/j.rse.2014.06.027

Mannino A, Novak MG, Nelson NB et al (2019) Measurement protocol of absorption by chromophoric dissolved organic matter (CDOM) and other dissolved materials. IOCCG Ocean Opt Biogeochem Protoc Satell Ocean Colour Sens Valid 1:1–77

Neubauer E, Köhler SJ, Von Der Kammer F et al (2013) Effect of pH and stream order on iron and arsenic speciation in boreal catchments. Environ Sci Technol 47:7120–7128. https://doi.org/10.1021/es401193j

Poulin BA, Ryan JN, Aiken GR (2014) Effects of iron on optical properties of dissolved organic matter. Environ Sci Technol 48:10098–10106. https://doi.org/10.1021/es502670r

Raymond PA, Saiers JE (2010) Event controlled DOC export from forested watersheds. Biogeochemistry 100:197–209. https://doi.org/10.1007/s10533-010-9416-7

Ries III KG, Newson JK, Smith MJ, et al (2017) StreamStats, version 4. Reston, VA

Sherman DM, Waite TD (1985) Electronic spectra of Fe^{3+} oxides and oxide hydroxides in the near IR to near UV. Am Mineral 70:1262–1269

Shultz M, Pellerin B, Aiken GR et al (2018) High frequency data exposes nonlinear seasonal controls on dissolved organic matter in a large watershed. Environ Sci Technol 52:5644–5652

Spencer RGM, Coble PG (2014) Sampling design for organic matter fluorescence analysis. Aquat Org Matter Fluoresc. https://doi.org/10.1017/cbo9781139045452.008

Spencer RGM, Bolton L, Baker A (2007) Freeze/thaw and pH effects on freshwater dissolved organic matter fluorescence and absorbance properties from a number of UK locations. Water Res 41:2941–2950. https://doi.org/10.1016/j.watres.2007.04.012

Stedmon CA, Markager S, Bro R (2003) Tracing dissolved organic matter in aquatic environments using a new approach to fluorescence spectroscopy. Mar Chem 82:239–254. https://doi.org/10.1016/S0304-4203(03)00072-0

Stefánsson A (2007) Iron(III) hydrolysis and solubility at 25 °C. Environ Sci Technol 4:6117–6123. https://doi.org/10.1021/es070174h

Stolpe B, Guo L, Shiller AM, Hassellöv M (2010) Size and composition of colloidal organic matter and trace elements in the Mississippi River, Pearl River and the northern Gulf of Mexico, as characterized by flow field-flow fractionation. Mar Chem 118:119–128. https://doi.org/10.1016/j.marchem.2009.11.007

Stolpe B, Guo L, Shiller AM, Aiken GR (2012) Abundance, size distributions and trace-element binding of organic and iron-rich nanocolloids in Alaskan rivers, as revealed by field-flow fractionation and ICP-MS. Geochim Cosmochim Acta 105:221–239. https://doi.org/10.1016/j.gca.2012.11.018

Taka M, Aalto J, Virkanen J, Luoto M (2016) The direct and indirect effects of watershed land use and soil type on stream water metal concentrations. Water Resour Res 52:7711–7725. https://doi.org/10.1002/2016WR019226

U.S. Geological Survey (2021) USGS Water Data for the Nation: U.S. Geological Survey National Water Information System Database. https://doi.org/10.5066/F7P55KJN. accessed 8 May 2021

U.S. Geological Survey (2022) USGS Watershed Boundary Dataset (WBD) for 2-digit Hydrologic Unit (published 20220118). https://www.sciencebase.gov/catalog/item/59d58b22e4b05fe04cc53863. accessed 9 Feb 2022

Wang W, Chen M, Guo L, Wang WX (2017) Size partitioning and mixing behavior of trace metals and dissolved organic matter in a South China estuary. Sci Total Environ 603–604:434–444. https://doi.org/10.1016/j.scitotenv.2017.06.121

Weishaar JL, Aiken GR, Bergamaschi BA et al (2003) Evaluation of specific ultraviolet absorbance as an indicator of the chemical composition and reactivity of dissolved organic carbon. Environ Sci Technol 37:4702–4708. https://doi.org/10.1021/es030360x

Wetzel RG (1992) Gradient-dominated ecosystems: sources and regulatory functions of dissolved organic matter in freshwater ecosystems. Hydrobiologia 92:181–198

Weyhenmeyer GA, Prairie YT, Tranvik LJ (2014) Browning of boreal freshwaters coupled to carbon-iron interactions along the aquatic continuum. PLoS ONE. https://doi.org/10.1371/journal.pone.0088104

Wilson HF, Xenopoulos MA (2008) Effects of agricultural land use on the composition of fluvial dissolved organic matter. Nat Geosci 2:37–41. https://doi.org/10.1038/ngeo391

Xiao YH, Sara-Aho T, Hartikainen H, Vähätalo AV (2013) Contribution of ferric iron to light absorption by chromophoric dissolved organic matter. Limnol Oceanogr 58:653–662. https://doi.org/10.4319/lo.2013.58.2.0653

Xiao Y-H, Räike A, Hartikainen H, Vähätalo AV (2015) Iron as a source of color in river waters. Sci Total Environ 536:914–923. https://doi.org/10.1016/j.scitotenv.2015.06.092

Zhang H, Yao B, Wang S, Wang G (2021) Remote sensing estimation of the concentration and sources of coloured dissolved organic matter based on MODIS: a case study of Erhai lake. Ecol Indic 131:108180. https://doi.org/10.1016/j.ecolind.2021.108180

Zhou Z, Stolpe B, Guo L, Shiller AM (2016) Colloidal size spectra, composition and estuarine mixing behavior of DOM in river and estuarine waters of the northern Gulf of Mexico. Geochim Cosmochim Acta 181:1–17. https://doi.org/10.1016/j.gca.2016.02.032

Publisher's Note Springer Nature remains neutral with regard to jurisdictional claims in published maps and institutional affiliations.